

# Event topology and constituent-quark scaling of elliptic flow in heavy-ion collisions at the Large Hadron Collider using a multiphase transport model

Neelkamal Mallick<sup>1</sup>, Sushanta Tripathy<sup>2</sup>, and Raghunath Sahoo<sup>1,3\*</sup>

<sup>1</sup>*Department of Physics, Indian Institute of Technology Indore, Simrol, Indore 453552, India*

<sup>2</sup>*INFN - sezione di Bologna, via Irnerio 46, 40126 Bologna BO, Italy and*

<sup>3</sup>*CERN, CH 1211, Geneva 23, Switzerland*

(Dated: May 21, 2021)

Transverse sphericity is an event shape observable, which has got a unique capability to separate the events based on their geometrical shapes. In this work, we use transverse sphericity to study the identified light flavor production in heavy-ion collisions using A Multi-Phase Transport (AMPT) model. We obtain the elliptic flow coefficients for pions, kaons and protons in Pb-Pb collisions at  $\sqrt{s_{NN}} = 5.02$  TeV as a function of transverse sphericity and collision centrality. Also, we study the number of constituent-quark (NCQ) scaling of elliptic flow which interprets the dominance of the quark degrees of freedom at early stages of the collision. We observe a clear dependence of the elliptic flow for identified particles on transverse sphericity. It is found that the NCQ-scaling is strongly violated in events with low transverse sphericity compared to transverse sphericity-integrated events.

PACS numbers:

## I. INTRODUCTION

The ultra-relativistic heavy-ion collisions at particle accelerators like the Large Hadron Collider (LHC) at CERN, Switzerland and Relativistic Heavy-Ion Collider (RHIC) at BNL, USA, provide signatures of possible formation of a deconfined state of quarks and gluons, known as Quark Gluon Plasma (QGP). Although, one does not observe any direct evidence of possible QGP formation due to its very short lifetime, instead several indirect signatures such as direct photon measurements, jet-quenching, elliptic flow ( $v_2$ ), strangeness enhancement, quarkonia suppression etc. suggest that formation of QGP is highly probable in such collisions. Due to the unprecedented energy scale of a few TeV, some of the QGP signatures [1, 2] are also observed in smallest collision systems (i.e. proton-proton collisions) at the LHC. To understand the underlying dynamics of small collision systems, an event shape observable, transverse sphericity, has been introduced recently [3–7] at the LHC energies. From these studies, it was observed that transverse sphericity has a very unique capability to separate the events based on their geometrical shapes, i.e. isotropic and jetty events [8, 9]. After its successful implementation in small collision systems, transverse sphericity can be used as a tool for heavy-ion collisions to differentiate events based on their event topology, even the environment is much more complex. It might reveal new and unique results from heavy-ion collisions where the production of a QGP medium is already established. In one of our recent publications [10], we have explicitly used transverse sphericity in heavy-ion collisions for the first time to study the azimuthal anisotropy of unidentified

charged particles as a function of transverse sphericity in A Multi-Phase Transport (AMPT) model. We observe a strong anti-correlation of transverse sphericity with the ellipticity of the events in heavy-ion collisions. It was found that high transverse sphericity events have nearly zero  $v_2$  while low transverse sphericity events contribute significantly to the  $v_2$ .

$v_2$  is generally caused by the initial spatial anisotropy in the system produced in a non-central collision. It plays a significant role to understand the collective motion and bulk property of the QGP.  $v_2$  is defined as the second-order Fourier component of the particle azimuthal distribution, which provides information of the transport properties of created medium in heavy-ion collisions [11]. The comparison of  $v_2$  measurements to hydrodynamic calculations reveal that the elliptic flow is built up mainly during the early partonic stages of QGP and it is governed by the evolution of QGP [12–16]. However, the hadronic rescattering in the hadronic phase could also contribute to the evolution of elliptic flow [17]. Thus, to understand the interplay of partonic versus hadronic phase in the evolution of elliptic flow, it is important to study the elliptic flow of different identified particles.

In addition, RHIC and LHC experimental results found that in the intermediate transverse momentum range, the  $v_2$  of baryons is larger than that of mesons [12]. Ref. [18] suggests that this phenomenon could be explained by the development of hydrodynamic flow in the partonic phase and then quarks coalesce into hadrons during the hadronization. This mechanism leads to number of constituent quarks (NCQ) scaling, a hierarchy observed in the values of  $v_2$  as a function of transverse momentum, where flow might no longer be dominant and this may compete with the contribution from jet fragmentation. This scaling property has been studied extensively in experiments [12, 19–21] and in theoretical studies [22–24]. Some of these results suggest that the

---

\*Corresponding author: *Raghunath.Sahoo@cern.ch*

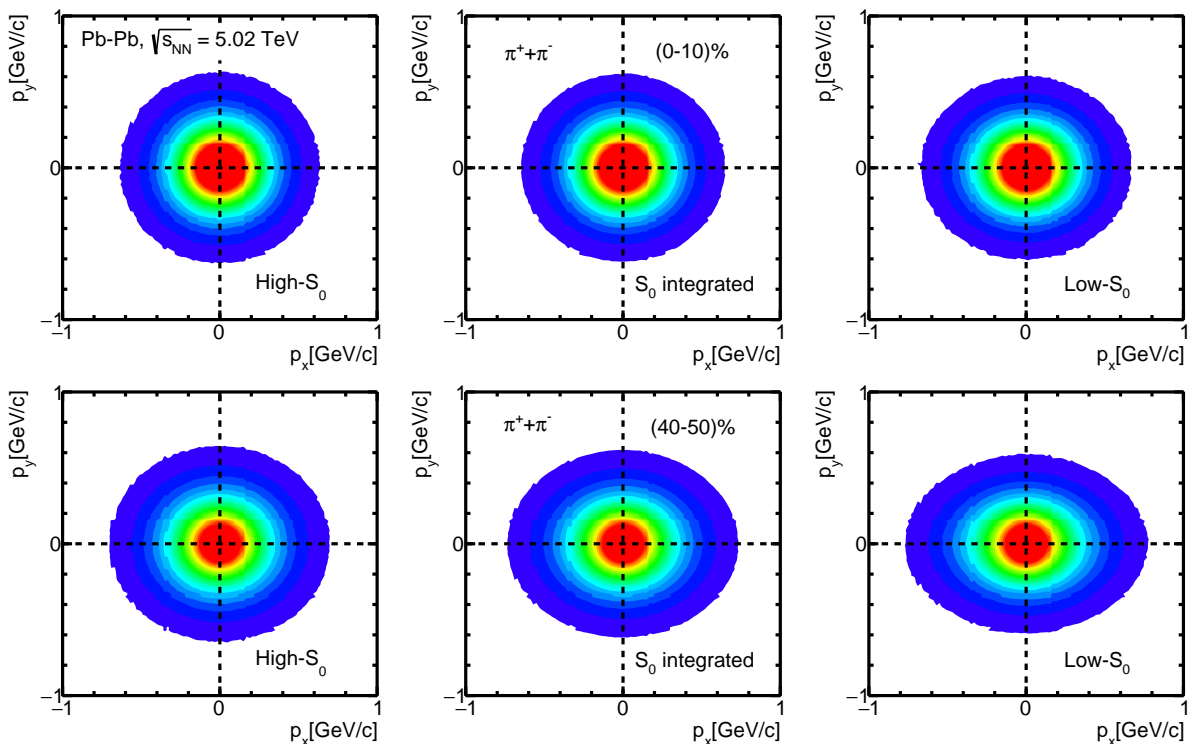


FIG. 1: (Color Online) Transverse momentum space correlation ( $p_y$  vs.  $p_x$ ) for  $\pi^+ + \pi^-$  in different sphericity classes for (0-10)% (top) and (40-50)% (bottom) central Pb-Pb collisions at  $\sqrt{s_{NN}} = 5.02$  TeV in AMPT model.

NCQ scaling of  $v_2$  at the LHC energies is violated [12, 21] for intermediate or high transverse momenta. It would be very interesting to study these properties of  $v_2$  in different event shapes. In this work, we obtain the transverse momentum spectra, two-particle correlations and elliptic flow of identified particles as a function of transverse sphericity in Pb-Pb collisions at  $\sqrt{s_{NN}} = 5.02$  TeV using AMPT model. We believe that the results would motivate experimentalists to pursue such a novel method in experiments at the LHC. In fact, in a recent study it has been shown that how machine learning tools can be implemented in experiments to obtain transverse sphericity [25].

The paper is organised as follows. We begin with a brief introduction and motivation for the study in Section I. In Section II, the detailed analysis methodology along with brief description about AMPT are given. Section III discusses about the results and finally they are summarized in Section IV.

## II. EVENT GENERATION AND ANALYSIS METHODOLOGY

In this section, we begin with a brief introduction on AMPT model and then we proceed with defining transverse sphericity and elliptic flow.

### A. A Multi-Phase Transport (AMPT) Model

AMPT model contains four components namely, initialization, parton transport, hadronization mechanism and hadron transport [26]. The initialization of the collisions is performed using HIJING [27], where the differential cross-section of the produced mini-jets in  $pp$  collisions is calculated. Then, the produced partons calculated in  $pp$  collisions is converted into  $p$ -A and heavy-ion collisions by parametrized shadowing function and nuclear overlap function with inbuilt Glauber model. The initial low-momentum partons are produced from parametrized coloured string fragmentation mechanisms and they are separated from high momentum partons by a momentum cut-off. The produced partons are propagated into parton transport part via Zhang's Parton Cascade (ZPC) model [28]. In the String Melting version of AMPT, melting of colored strings into low momentum partons takes place at the start of the ZPC. It is calculated using Lund FRITIOF model of HIJING. The resulting partons undergo multiple scatterings which take place when any two partons are within a distance of minimum approach. In AMPT-SM, the transported partons are finally hadronized using spatial coalescence mechanism [29, 30]. The produced hadrons further undergo final evolution in a relativistic transport mechanism [31, 32] via meson-meson, meson-baryon and baryon-baryon interactions. There is also a default ver-

sion of AMPT, where instead of coalescing the partons, fragmentation mechanism using Lund fragmentation parameters  $a$  and  $b$  are used for hadronizing the transported partons. However, the particle flow and spectra at the mid- $p_T$  regions are well explained by quark coalescence mechanism for hadronization [33–35]. Thus, we have used string melting mode of AMPT (AMPT version 2.26t9b) for all of our calculations in the current work. The AMPT settings in the current work, are the same as reported in Refs. [10, 36]. One should note that, to exactly match with the experimental data, one can vary the tunes of the AMPT model, which is currently out of the scope of this manuscript. For the input of impact parameter values for different centralities in Pb-Pb collisions, we have used Ref. [37].

### B. Transverse Sphericity

Transverse sphericity is an event property which is defined for a unit vector  $\hat{n}(n_T, 0)$  that minimizes the ratio [3, 4]:

$$S_0 = \frac{\pi^2}{4} \left( \frac{\sum_i |\vec{p}_{T_i} \times \hat{n}|}{\sum_i p_{T_i}} \right)^2. \quad (1)$$

By restricting it to the transverse plane, transverse sphericity becomes infrared and collinear safe [5]. By construction, the extreme limits of transverse sphericity are related to specific configurations of events in transverse plane i.e. jetty and isotropic. The value of transverse sphericity ranges from 0 to 1, which is ensured by multiplying the normalization constant  $\pi^2/4$  in Eq. 1. Here onwards, for the sake of simplicity the transverse sphericity is referred as sphericity. To disentangle the low- $S_0$  and high- $S_0$  events from the sphericity-integrated events, we have applied sphericity cuts on the generated events. The sphericity distributions are selected in the pseudo-rapidity range of  $|\eta| < 0.8$  with a minimum constraint of 5 charged particles with  $p_T > 0.15$  GeV/c to recreate conditions similar to ALICE experiment at the LHC. The low- $S_0$  events are those events having sphericity values in the lowest 20% and the high- $S_0$  events are those occupying the highest 20% in the sphericity distribution. The sphericity cuts are shown in Table I.

TABLE I: Lowest 20 % (low- $S_0$ ) and highest 20% (high- $S_0$ ) cuts on sphericity distribution.

Centrality (%)	low- $S_0$	high- $S_0$
0-10	0-0.88025	0.95285-1
40-50	0-0.71475	0.86365-1
60-70	0-0.70775	0.87355-1

Figure 1 shows the transverse momentum space correlation ( $p_y$  vs.  $p_x$ ) for  $\pi^+ + \pi^-$  in different sphericity

classes for (0-10)% (top) and (40-50)% (bottom) central Pb-Pb collisions at  $\sqrt{s_{NN}} = 5.02$  TeV in AMPT model. The sphericity integrated events for (40-50)% centrality class clearly show anisotropy in the momentum space which is linked to the initial state geometrical anisotropy. However such an anisotropy is not observed in the (0-10)% centrality class. This behavior is understood as semi-central collisions develop an almond shape of nuclear overlap region in the initial stage while for most central collisions the nuclear overlap region is nearly circular. When one studies the transverse momentum space correlation in different sphericity classes, the low- $S_0$  events show higher anisotropy compared to sphericity-integrated events while high- $S_0$  events show nearly zero anisotropy. This is one of the testimonies that sphericity is a unique tool for the event classification to study the particle production in heavy-ion collisions.

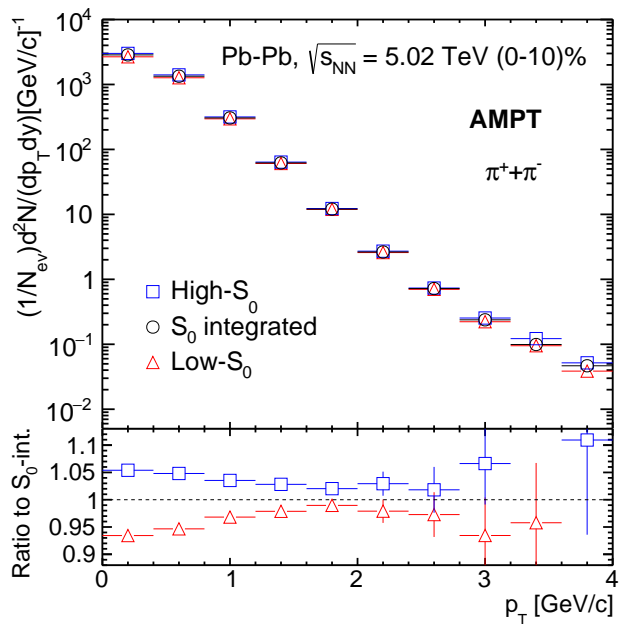


FIG. 2: (Color Online) Top plot:  $p_T$ -spectra for pions in (0-10)% central Pb-Pb collisions for high- $S_0$ ,  $S_0$ -integrated and low- $S_0$  classes. Bottom plot: Ratio of  $p_T$ -spectra for high- $S_0$  and low- $S_0$  events to the  $S_0$ -integrated events.

### C. Elliptic Flow

In non-central heavy-ion collisions, the initial spatial anisotropies of the nuclear overlap region gets converted to the final state momentum space azimuthal anisotropy of the produced hadrons due to the strong differential pressure gradients of the QGP medium. The observed non-zero finite azimuthal anisotropy (evident from Fig. 1) can be expressed as a Fourier series in the azimuthal an-

gle,  $\phi$ :

$$E \frac{d^3 N}{dp^3} = \frac{d^2 N}{2\pi p_T dp_T dy} \left( 1 + 2 \sum_{n=1}^{\infty} v_n \cos[n(\phi - \psi_n)] \right). \quad (2)$$

Here,  $v_n$  is the magnitude of anisotropic flow of different order  $n$ , and  $\psi_n$  is the  $n^{\text{th}}$  harmonic event plane angle [38].  $v_n$  is usually studied as a function of transverse momentum ( $p_T$ ) and pseudorapidity ( $\eta$ ).

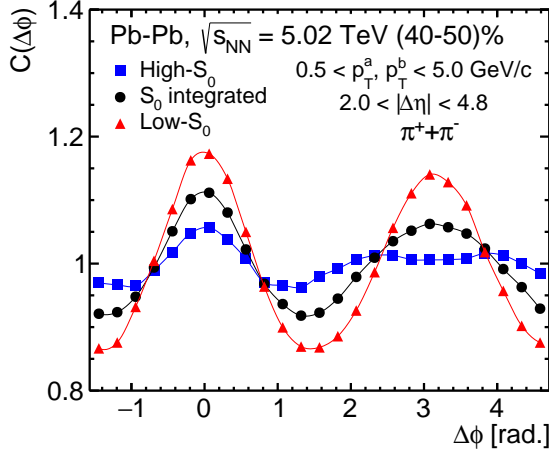


FIG. 3: (Color Online) One dimensional azimuthal correlation of pions for low- $S_0$  (red triangles), high- $S_0$  (blue squares) and sphericity-integrated (black circles) events in 40-50% central Pb-Pb collisions at  $\sqrt{s_{\text{NN}}} = 5.02$  TeV using AMPT model.

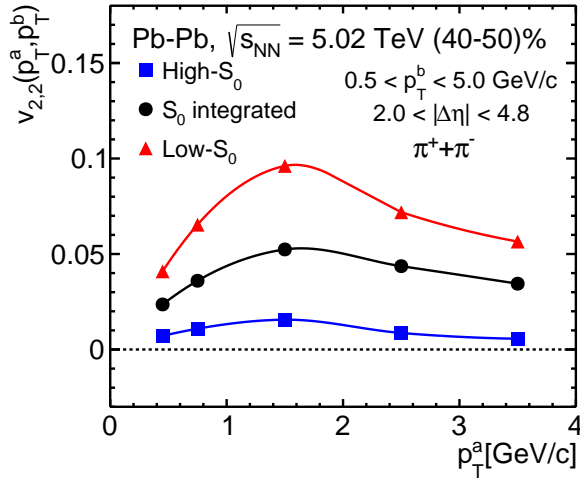


FIG. 4: (Color Online) Two particle elliptic flow coefficients of pions for low- $S_0$  (red triangles), high- $S_0$  (blue squares) and sphericity-integrated (black circles) events in 40-50% central Pb-Pb collisions at  $\sqrt{s_{\text{NN}}} = 5.02$  TeV using AMPT model.

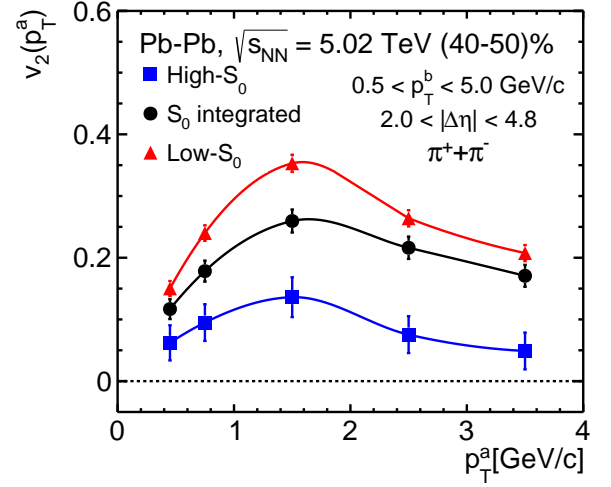


FIG. 5: (Color Online) Single particle elliptic flow coefficients of pions for low- $S_0$  (red triangles), high- $S_0$  (blue squares) and sphericity-integrated (black circles) events in 40-50% central Pb-Pb collisions at  $\sqrt{s_{\text{NN}}} = 5.02$  TeV using AMPT model.

For  $n = 2$ , Eq. 2 gives the second order harmonics in the expansion and its coefficient,  $v_2$  provides the numerical measure of the elliptic flow which is defined as:

$$v_2 = \langle \cos(2(\phi - \psi_2)) \rangle \quad (3)$$

Due to the almond shaped nuclear overlap region in a non-central heavy-ion collision, the azimuthal anisotropy is expected to be dominated by the  $v_2$  component. In addition, the signatures of  $v_1$  (directed flow) and  $v_3$  (triangular flow) are observed but their contribution is quite less as compared to  $v_2$ . Another interesting observable owing to anisotropic flow and properties of the medium is the correlation function between two particles in relative pseudorapidity ( $\Delta\eta = \eta_a - \eta_b$ ) and azimuthal angle ( $\Delta\phi = \phi_a - \phi_b$ ). The labels  $a$  and  $b$  denote the two particles in the pair, which are chosen from different (or same) transverse momentum intervals. In this study, we have taken particles in  $|\eta| < 2.5$  to include wider range of particles mostly contributing to  $v_2$  and  $p_T > 0.5$  GeV/c to be consistent with Refs. [10, 39]. The two particle correlation function,  $C(\Delta\eta, \Delta\phi)$  can be constructed as the ratio of distributions for same-event pairs,  $S(\Delta\eta, \Delta\phi)$  and mixed-event pairs,  $B(\Delta\eta, \Delta\phi)$ , which is given by:

$$C(\Delta\eta, \Delta\phi) = \frac{S(\Delta\eta, \Delta\phi)}{B(\Delta\eta, \Delta\phi)} \quad (4)$$

We have chosen five randomly selected events for the mixed-event pairing and hence the pairs contain no physical correlations whatsoever. To obtain the anisotropy in azimuthal direction, our analysis focuses mainly on the

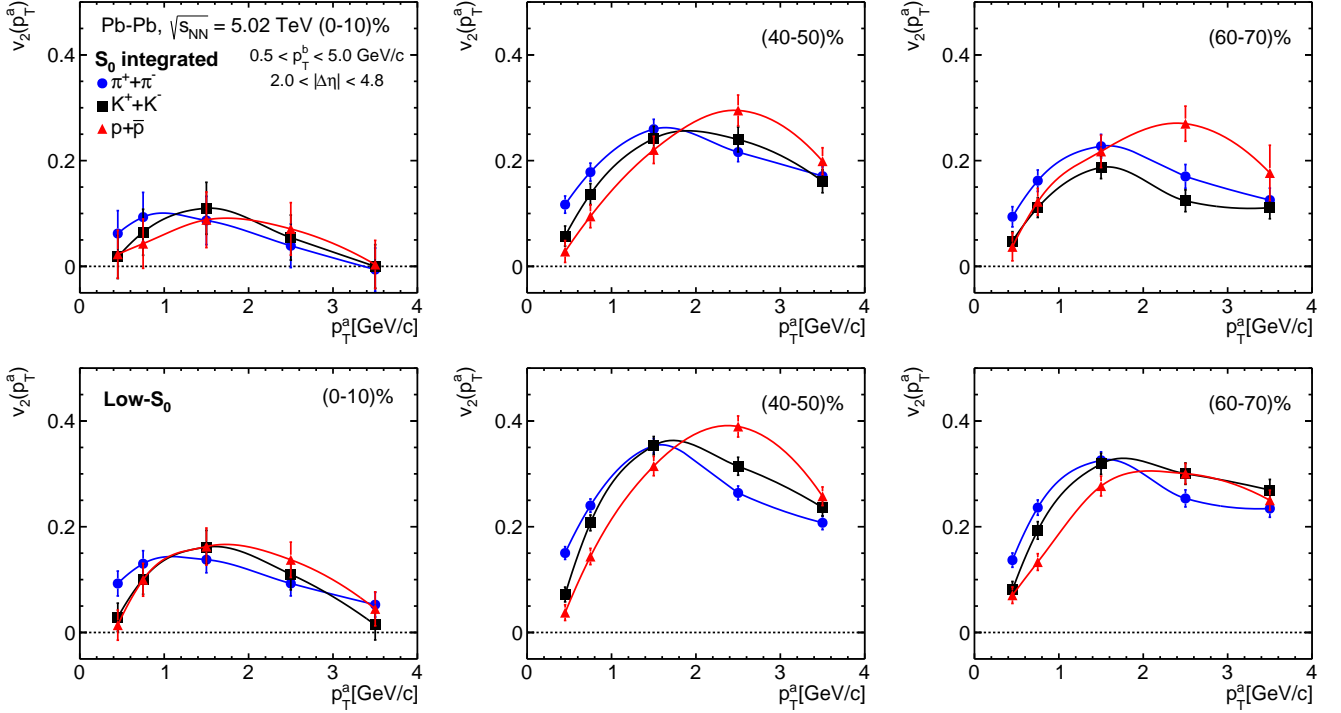


FIG. 6: (Color Online) Centrality dependence of elliptic flow co-efficient ( $v_2(p_T^a)$ ) as a function of  $p_T^a$  of pions (blue circles), kaons (black squares) and protons (red triangles) for sphericity-integrated (top panel) and low- $S_0$  (bottom panel) events in Pb-Pb collisions at  $\sqrt{s_{NN}} = 5.02$  TeV using AMPT model.

shape of the 1D correlation function  $\Delta\phi$ , given as;

$$C(\Delta\phi) = \frac{dN_{\text{pairs}}}{d\Delta\phi} = A \times \frac{\int S(\Delta\eta, \Delta\phi) d\Delta\eta}{\int B(\Delta\eta, \Delta\phi) d\Delta\eta}. \quad (5)$$

Here, the normalization constant  $A$  ensures that the number of pairs to be the same between the signal ( $S$ ) and background ( $B$ ) events for a given  $\Delta\eta$  interval. The  $\Delta\eta$  interval is chosen carefully by excluding the jet peak region observed in the  $C(\Delta\eta, \Delta\phi)$  distribution. For our case, the interval is taken to be  $2.0 < |\Delta\eta| < 4.8$ . By choosing particle pairs with a proper pseudorapidity cut, the two-particle correlation method removes the residual non-flow effects in the estimation of elliptic flow. Non-flow azimuthal correlations usually arise from jets and short range resonance decays, which are not associated with the symmetry planes at the early stage of the collisions. Although the non-flow effects are very small in heavy-ion collisions at very high energies, but our study based on event shape dependence being sensitive to jets may get affected by these effects and hence we proceed with this method. To ensure the consistency of the method, one can have a look at Fig. 3 of Ref. [10], where the comparison of calculated  $v_{2,2}$  between PYTHIA8 (Angantyr) [40] and AMPT model is shown. It is shown that the method removes residual non-flow contributions without affecting the event shape studies based on transverse sphericity. Now, the pair distribu-

tion ( $N_{\text{pairs}}$ ) can be expanded in  $\Delta\phi$  into a Fourier series:

$$\frac{dN_{\text{pairs}}}{d\Delta\phi} \propto \left[ 1 + 2 \sum_{n=1}^{\infty} v_{n,n}(p_T^a, p_T^b) \cos n\Delta\phi \right]. \quad (6)$$

Here,  $v_{n,n}$  is called as the two particle flow coefficient. By rewriting Eq. 6 with the help of Eq. 5 one obtains:

$$C(\Delta\phi) \propto \left[ 1 + 2 \sum_{n=1}^{\infty} v_{n,n}(p_T^a, p_T^b) \cos n\Delta\phi \right]. \quad (7)$$

Now,  $v_{n,n}$  can be calculated as:

$$v_{n,n}(p_T^a, p_T^b) = \langle \cos(n\Delta\phi) \rangle \quad (8)$$

We have taken very narrow bins in  $-\pi/2 < \Delta\phi < 3\pi/2$ .  $v_{n,n}$  are symmetric functions with respect to  $p_T^a$  and  $p_T^b$ . The definition of harmonics defined in Eq. 2 also enters in Eq. 6, which can be rewritten as;

$$\frac{dN_{\text{pairs}}}{d\Delta\phi} \propto \left[ 1 + 2 \sum_{n=1}^{\infty} v_n(p_T^a) v_n(p_T^b) \cos n\Delta\phi \right]. \quad (9)$$

By this definition, the event plane angle drops out in convolution. So, if the azimuthal anisotropy is driven by collective expansion then  $v_{n,n}$  should factorize into the

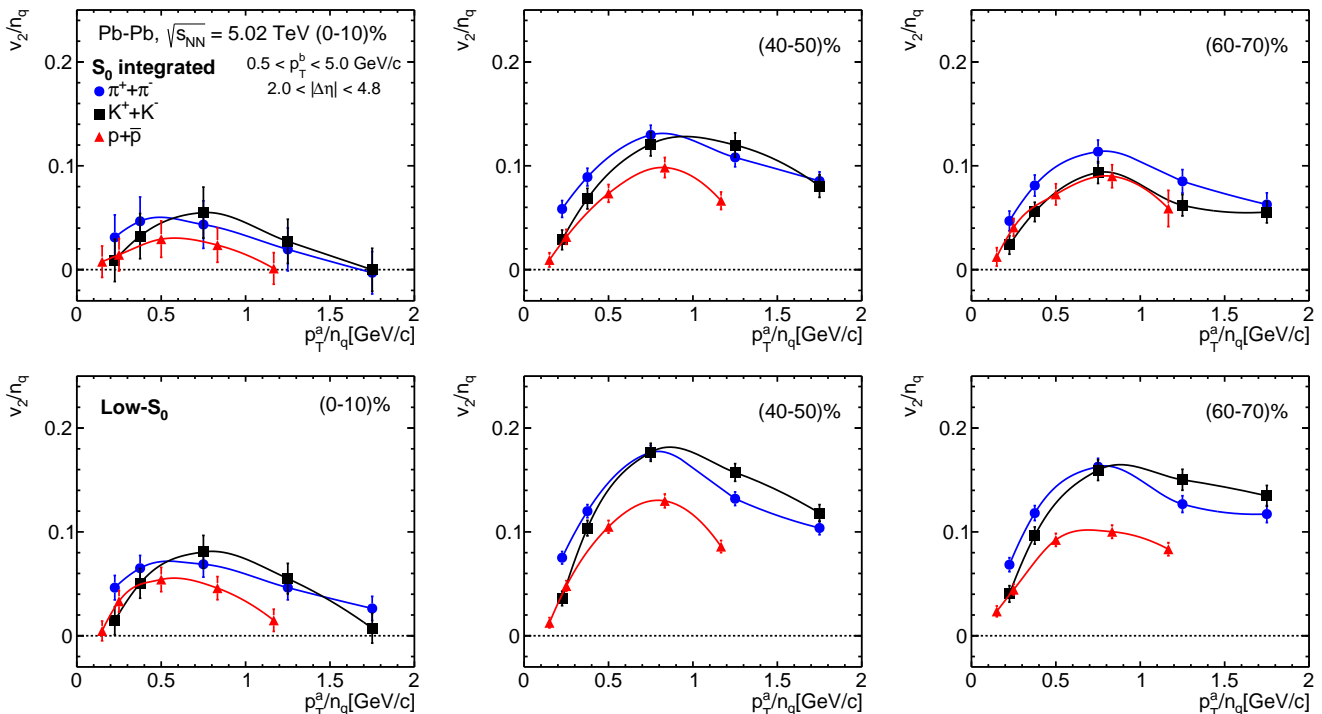


FIG. 7: (Color Online) Centrality dependence of elliptic flow co-efficient with number of quark participant scaling ( $v_2(p_T^a)/n_q$ ) as a function of  $p_T^a$  of pions (blue circles), kaons (black squares) and protons (red triangles) for sphericity-integrated (top panel) and low- $S_0$  (bottom panel) events in Pb-Pb collisions at  $\sqrt{s_{NN}} = 5.02$  TeV using AMPT model.

product of two single-particle harmonic coefficients.

$$v_{n,n}(p_T^a, p_T^b) = v_n(p_T^a)v_n(p_T^b). \quad (10)$$

From Eq. 10 we derive the single particle flow coefficient as:

$$v_n(p_T^a) = v_{n,n}(p_T^a, p_T^b) / \sqrt{v_{n,n}(p_T^b, p_T^b)} \quad (11)$$

We now proceed for the estimation of azimuthal anisotropy of  $\pi^+ + \pi^-$ ,  $K^+ + K^-$  and  $p + \bar{p}$  in different sphericity classes for Pb-Pb collisions at the LHC energies from AMPT. For better readability, here onwards we refer  $\pi^+ + \pi^-$ ,  $K^+ + K^-$  and  $p + \bar{p}$  as pions, kaons and protons, respectively.

### III. RESULTS AND DISCUSSIONS

Top panel of Fig. 2 shows the  $p_T$ -spectra for pions in (0-10)% Pb-Pb collisions for high- $S_0$ ,  $S_0$ -integrated and low- $S_0$  events and bottom panel shows the ratio of  $p_T$ -spectra for high- $S_0$  and low- $S_0$  events to the  $S_0$ -integrated events. In the low- $p_T$  region, we observe that pion production is dominated by high- $S_0$  events. But as we move on to higher  $p_T$ , the relative yield from high- $S_0$  and low- $S_0$  events are similar. These results show that sphericity successfully differentiates the heavy-ion collisions event

topology based on their geometrical shapes i.e. high- $S_0$  and low- $S_0$ .

Figure 3 shows one dimensional azimuthal correlation of pions for low- $S_0$ , high- $S_0$  and sphericity-integrated events in 40-50% central Pb-Pb collisions at  $\sqrt{s_{NN}} = 5.02$  TeV. As described in the previous section, the correlation function is calculated in the  $p_T$  range of 0.5 to 5 GeV/c for  $2.0 < |\Delta\eta| < 4.8$ . We see a strong correlation of modulation magnitude with sphericity in Fig. 3. Also, double peak is observed for away side ( $\Delta\phi \sim \pi$ ) for high- $S_0$  events, which may arise from the residual contribution of the triangular flow. The observed behavior is analogous to the behavior observed in Refs. [39], where flow vector is used as an event classifier for heavy-ion collisions. Figures 4 and 5 show the two particle and single particle elliptic flow coefficients of pions for low- $S_0$ , high- $S_0$  and sphericity-integrated events in 40-50% central Pb-Pb collisions at  $\sqrt{s_{NN}} = 5.02$  TeV obtained using Eqs. 8 and 11, respectively. We observe that the contribution towards elliptic flow coefficients is dominated by low- $S_0$  events while high- $S_0$  events show nearly zero elliptic flow coefficients. In a similar fashion, we obtain the elliptic flow coefficients for pions, kaons and protons and then study the number of constituent quark scaling (NCQ) of the elliptic flow coefficients.

Figure 6 shows the single particle elliptic flow coefficient ( $v_2(p_T^a)$ ) as a function of  $p_T^a$  for pions, kaons and protons in (0-10)%, (40-50)% and (60-70)% central

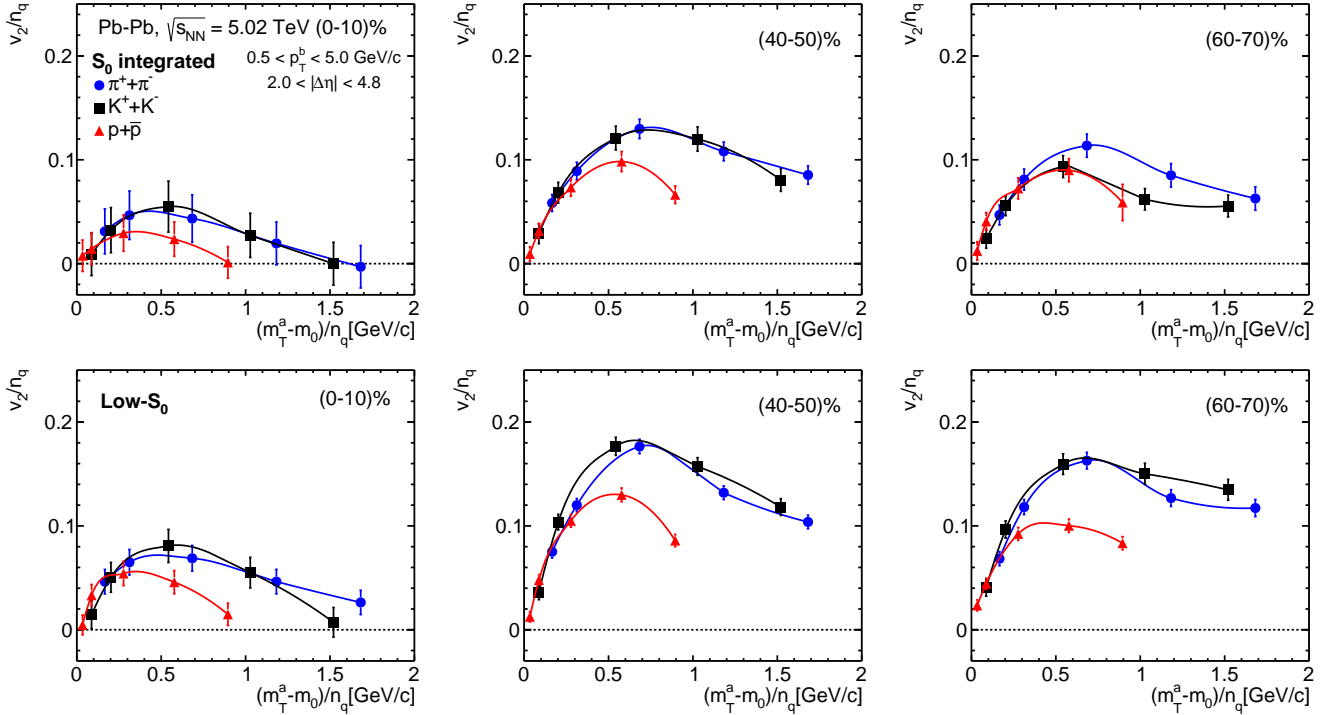


FIG. 8: (Color Online) Centrality dependence of elliptic flow co-efficient with transverse mass ( $m_T$ ) scaling as a function of  $p_T^a$  of pions (blue circles), kaons (black squares) and protons (red triangles) for spherocity-integrated (top panel) and low- $S_0$  (bottom panel) events in Pb-Pb collisions at  $\sqrt{s_{NN}} = 5.02$  TeV using AMPT model.

Pb-Pb collisions at  $\sqrt{s_{NN}} = 5.02$  TeV for spherocity-integrated and low- $S_0$  classes. The values of  $v_2(p_T^a)$  increases from (0-10)% to (40-50)% central collisions while slightly decreases for (60-70)% central collisions for all particle species. The increasing behavior is consistent with the picture of geometry of the collision driving the final state anisotropy. The slight decrease for (60-70)% central collisions might have originated from an interplay of different effects like the smaller lifetime of the fireball in peripheral collisions with respect to most central collisions which does not allow the elliptic flow to further develop and less significant contribution of eccentricity fluctuations and to final state hadronic effects [41]. For (40-50)% and (60-70)% central collisions, we see a clear mass hierarchy in the low- $p_T$  region ( $p_T < 2$  GeV/c) and in the intermediate- $p_T$  the elliptic flow for protons are higher than that of pions and kaons. As per hydrodynamic calculations, the mass hierarchy in the low- $p_T$  could be an interplay between radial and elliptic flow. The baryon and meson separation in the intermediate- $p_T$  could arise from the quark coalescence mechanism of AMPT string melting mode. As described earlier, in the string melting mode of AMPT, when a quark and an anti-quark are close in phase space with their momenta very close to each other, they coalesce to form a meson. When three quarks come closer in phase space, they combine to form a baryon. Thus the probability of recombination of three quarks becomes higher in the intermediate- $p_T$

range.

Owing to the quark coalescence mechanism, one may expect elliptic flow to follow the constituent quark number (NCQ) scaling behavior. If elliptic flow follows NCQ-scaling, then it can be expressed as,

$$v_2^h(p_T^a) = n_q \times v_2^a(p_T^a/n_q). \quad (12)$$

Here,  $n_q$  is the number of constituent quarks for h-hadron. In RHIC experimental observations [19, 20, 42], it was found that the identified particles follow the NCQ scaling behavior. The PHENIX collaboration extends the scaling property to the lower transverse momentum by obtaining elliptic flow as a function of the transverse kinetic energy, where the kinetic energy is defined by  $m_T - m_0$  [20, 43, 44]. Here,  $m_T$  is the transverse mass ( $\sqrt{p_T^2 + m_0^2}$ ) and  $m_0$  is the rest mass of the particle. The kinetic energy representation of scaling was found to be valid in the RHIC results. Also, this scaling behavior was successfully reproduced by models which invokes quark coalescence as the dominant hadronization mechanism [22–24, 45]. Thus, the NCQ scaling of the elliptic flow has been interpreted as evidence of the dominance of quark degrees of freedom in the initial stages of heavy-ion collisions [22–24, 45]. In this work, we have studied both the NCQ-scaling behavior for pions, kaons and protons. Figure 7 shows centrality dependence of elliptic flow co-efficient with number of quark participant scal-

ing  $(v_2(p_T^a)/n_q)$  as a function of  $p_T^a/n_q$  of pions, kaons and protons for spherocity-integrated and low- $S_0$  events. Figure 8 shows the transverse kinetic energy,  $v_2(p_T^a)/n_q$  scaling as a function of  $(m_T - m_0)/n_q$ . In the intermediate transverse momentum range, where the quark coalescence mechanism is dominant, both the scaling of  $v_2(p_T^a)/n_q$  show a significant deviation. Results from LHC suggests that both NCQ and transverse kinetic energy scaling of  $v_2(p_T^a)/n_q$  at the LHC energies show a deviation of 20% [12, 21] for intermediate/high transverse momenta. The observed deviations seems to be similar for all centrality classes.

Let us now discuss how the results vary when such a study is performed in different spherocity classes. In Fig. 6, for (0-10)% centrality we see that the values of  $v_2$  is similar in both spherocity-integrated and low- $S_0$  events. For (40-50)% and (60-70)% centrality classes we see significantly higher  $v_2$  in low- $S_0$  events compared to the spherocity-integrated events for all particles. For (40-50)% centrality class, the baryon-meson separation in intermediate- $p_T$  is more prominent in low- $S_0$  events compared to spherocity-integrated events. While studying the NCQ scaling and transverse kinetic energy scaling of the elliptic flow for different spherocity classes in Figs. 7 and 8, it was found that the low- $S_0$  events show a larger deviation compared to spherocity-integrated events in all centrality classes. The deviation is highly significant, where one can draw a conclusion of violation in the NCQ scaling of elliptic flow at the LHC energies in AMPT model. This essentially indicates that using spherocity not only one can study the events with enhanced elliptic flow but also one can directly probe into the scaling properties of the elliptic flow. Thus, spherocity can separate out the events where the initial stage of the systems is dominated by the quark degrees of freedom from total events. Such an observation strengthens our previous publications using simulation from AMPT model [10, 25], where it was argued that the transverse spherocity can be used as an event classifier in experimental analyses for heavy-ion collisions at RHIC and LHC.

#### IV. SUMMARY

In summary,

- The transverse momentum space correlation as a function of transverse spherocity indicates a strong correlation of transverse spherocity with the azimuthal anisotropy in the produced system in

heavy-ion collisions. This correlation is further confirmed with the study of transverse spherocity dependent one dimensional azimuthal correlation.

- The contribution towards elliptic flow coefficients is dominated by low- $S_0$  events while high- $S_0$  events show nearly zero elliptic flow.
- The baryon-meson separation at the intermediate transverse momentum, the NCQ scaling and the transverse kinetic energy scaling of  $v_2(p_T^a)/n_q$  from AMPT show a similar behavior for pions, kaons and protons as observed at the LHC.
- The baryon-meson separation in intermediate- $p_T$  was found to be more prominent in low- $S_0$  events compared to spherocity-integrated events.
- The study on the NCQ scaling and the transverse kinetic energy scaling of the elliptic flow in different spherocity classes shows that the low- $S_0$  events violate the scaling properties of the elliptic flow. This essentially indicates that using spherocity not only one can study the events with enhanced elliptic flow but also one can directly probe into the scaling properties of the elliptic flow.

One should note that these results are obtained from an event generator (AMPT) which successfully describes the elliptic flow for spherocity-integrated events in heavy-ion collisions. Thus it is expected that the observed behaviours to mimic the experimental data. However, any deviation of experimental results from AMPT results on elliptic flow could be very interesting to understand the system dynamics. We believe that in coming days of Run-3 at the LHC, transverse spherocity can serve as an important event classifier which could give a better insight to the possible QGP formation in heavy-ion collisions.

#### Acknowledgements

R.S. acknowledges the financial supports under the CERN Scientific Associateship and the financial grants under DAE-BRNS Project No. 58/14/29/2019-BRNS of the Government of India. S.T. acknowledges the supports under the INFN postdoctoral fellowship. The authors would like to acknowledge the usage of resources of the LHC grid Tier-3 computing facility at IIT Indore.

---

[1] J. Adam *et al.* [ALICE Collaboration], Nature Phys. **13**, 535 (2017).  
 [2] V. Khachatryan *et al.* [CMS Collaboration], Phys. Lett. B **765**, 193 (2017).  
 [3] E. Cuautle, R. Jimenez, I. Maldonado, A. Ortiz, G. Paic

and E. Perez, arXiv:1404.2372 [hep-ph].  
 [4] A. Ortiz, G. Paic and E. Cuautle, Nucl. Phys. A **941**, 78 (2015).  
 [5] G. P. Salam, Eur. Phys. J. C **67**, 637 (2010).  
 [6] G. Bencédi [ALICE Collaboration], Nucl. Phys. A **982**,

- 507 (2019)
- [7] A. Banfi, G. P. Salam and G. Zanderighi, *JHEP* **1006**, 038 (2010).
- [8] S. Tripathy, A. Bisht, R. Sahoo, A. Khuntia and M. P. Salvan, *Adv. High Energy Phys.* **2021**, 8822524 (2021).
- [9] A. Khuntia, S. Tripathy, A. Bisht and R. Sahoo, *J. Phys. G* **48**, 035102 (2021).
- [10] N. Mallick, R. Sahoo, S. Tripathy and A. Ortiz, *J. Phys. G* **48**, 045104 (2021).
- [11] S. Voloshin and Y. Zhang, *Z. Phys. C* **70**, 665 (1996).
- [12] B. B. Abelev *et al.* [ALICE Collaboration], *JHEP* **06**, 190 (2015).
- [13] I. Arsene *et al.* [BRAHMS Collaboration], *Nucl. Phys. A* **757**, 1 (2005).
- [14] K. Adcox *et al.* [PHENIX Collaboration], *Nucl. Phys. A* **757**, 184 (2005).
- [15] B. B. Back *et al.* [PHOBOS Collaboration], *Nucl. Phys. A* **757**, 28 (2005).
- [16] J. Adams *et al.* [STAR Collaboration], *Nucl. Phys. A* **757**, 102 (2005).
- [17] T. Hirano, U. W. Heinz, D. Kharzeev, R. Lacey and Y. Nara, *Phys. Lett. B* **636**, 299 (2006).
- [18] S. A. Voloshin, *Nucl. Phys. A* **715**, 379 (2003).
- [19] J. Adams *et al.* [STAR Collaboration], *Phys. Rev. Lett.* **92**, 052302 (2004).
- [20] S. S. Adler *et al.* [PHENIX Collaboration], *Phys. Rev. Lett.* **91**, 182301 (2003).
- [21] K. Aamodt *et al.* [ALICE Collaboration], *Phys. Rev. Lett.* **105**, 252302 (2010).
- [22] D. Molnar and S. A. Voloshin, *Phys. Rev. Lett.* **91**, 092301 (2003).
- [23] V. Greco, C. M. Ko and P. Levai, *Phys. Rev. C* **68**, 034904 (2003).
- [24] R. J. Fries, B. Muller, C. Nonaka and S. A. Bass, *Phys. Rev. C* **68**, 044902 (2003).
- [25] N. Mallick, S. Tripathy, A. N. Mishra, S. Deb and R. Sahoo, *Phys. Rev. D* (2021: In Press), arXiv:2103.01736 [hep-ph].
- [26] Z. W. Lin, C. M. Ko, B. A. Li, B. Zhang and S. Pal, *Phys. Rev. C* **72**, 064901 (2005).
- [27] X. N. Wang and M. Gyulassy, *Phys. Rev. D* **44**, 3501 (1991).
- [28] B. Zhang, *Comput. Phys. Commun.* **109**, 93 (1998).
- [29] Z. w. Lin and C. M. Ko, *Phys. Rev. C* **65**, 034904 (2002).
- [30] Y. He and Z. W. Lin, *Phys. Rev. C* **96**, 014910 (2017).
- [31] B. Li, A. T. Sustich, B. Zhang and C. M. Ko, *Int. J. Mod. Phys. E* **10**, 267 (2001).
- [32] B. A. Li and C. M. Ko, *Phys. Rev. C* **52**, 2037 (1995).
- [33] V. Greco, C. M. Ko and P. Levai, *Phys. Rev. C* **68**, 034904 (2003).
- [34] R. J. Fries, B. Muller, C. Nonaka and S. A. Bass, *Phys. Rev. Lett.* **90**, 202303 (2003).
- [35] R. J. Fries, B. Muller, C. Nonaka and S. A. Bass, *Phys. Rev. C* **68**, 044902 (2003).
- [36] S. Tripathy, S. De, M. Younus and R. Sahoo, *Phys. Rev. C* **98**, 064904 (2018).
- [37] C. Loizides, J. Kamin and D. d'Enterria, *Phys. Rev. C* **97**, 054910 (2018) Erratum: [*Phys. Rev. C* **99**, 019901 (2019)]
- [38] B. B. Abelev *et al.* [ALICE Collaboration], *JHEP* **1506**, 190 (2015).
- [39] G. Aad *et al.* [ATLAS Collaboration], *Phys. Rev. C* **92**, 034903 (2015).
- [40] C. Bierlich, G. Gustafson, L. Lönnblad and H. Shah, *JHEP* **10**, 134 (2018).
- [41] H. Song, S. Bass and U. W. Heinz, *Phys. Rev. C* **89**, 034919 (2014).
- [42] B. I. Abelev *et al.* [STAR Collaboration], *Phys. Rev. C* **75**, 054906 (2007).
- [43] S. Afanasiev *et al.* [PHENIX Collaboration], *Phys. Rev. Lett.* **99**, 052301 (2007).
- [44] A. Adare *et al.* [PHENIX Collaboration], *Phys. Rev. Lett.* **98**, 162301 (2007).
- [45] R. C. Hwa and C. B. Yang, *Phys. Rev. C* **70**, 024904 (2004).